Chemical Science

ROYAL SOCIETY OF CHEMISTRY

EDGE ARTICLE

View Article Online
View Journal | View Issue

Cite this: *Chem. Sci.*, 2020, **11**, 4779

All publication charges for this article have been paid for by the Royal Society of Chemistry

Received 22nd January 2020
Accepted 23rd April 2020

DOI: 10.1039/d0sc00409j

rsc.li/chemical-science

Expected and unexpected photoreactions of 9-(10-)substituted anthracene derivatives in cucurbit[*n*]uril hosts†

Xianchen Hu,[a] Fengbo Liu,[a] Xiongzhi Zhang,[ab] Zhiyong Zhao[ab] and Simin Liu *[ab]

By arranging substrates in a "reaction ready" state through noncovalent interactions, supramolecular nanoreactors/catalysts show high selectivity and/or rate acceleration features. Herein, we report the host–guest complexation of 9-(10-)substituted anthracene derivatives (**G1–G3**) with cucurbit[*n*]uril (CB[*n*], *n* = 8, 10), and the photoreactions of these derivatives in the presence of CB[*n*] hosts. Both CB[10] and CB[8] showed no obvious effects on the photoreaction of 9,10-disubstituted derivative **G1**. For **G2** and **G3**, CB[10] operated as either a nanoreactor or catalyst (10%) for the photodimerization of two compounds with high selectivity and high yield. However, although CB[8] formed a 1 : 2 complex with **G2**, as also observed with CB[10], the photosolvolysis product (9-anthracenemethanol) was obtained quantitatively after photoirradiation of the CB[8]·2**G2** complex. This unexpected photosolvolysis was rationalized by a plausible catalytic cycle in which anthracene acts as a photoremovable protecting group (PPG) and the carbonium ion intermediate is stabilized by CB[8].

Introduction

Inspired by natural enzymes, supramolecular nanoreactors/catalysts have been developed to achieve reactions with high selectivity and/or rate acceleration.[1,2] In host–guest chemistry, many types of macrocyclic host molecules have been explored as supramolecular nanoreactors/catalysts, such as cyclodextrins,[3] calixarenes,[4] pillararenes,[5] and nanocages, among others.[6–9] Photochemical reactions of anthracene and its derivatives, including anthracene dimerization and other unimolecular photoreactions, have been widely investigated over the last 100 years owing to the unique photo-responsive properties of these compounds.[10,11] However, the anthracene group acted as photoremovable protecting group (PPG) in only one example.[12,13] In supramolecular chemistry, host–guest interactions have been introduced to regulate the photodimerization of anthracene derivatives.[14–18] Furthermore, anthracene dimerization has been further used in the design of host–guest-related supramolecular polymers and optical materials/devices.[19–25]

Cucurbit[*n*]urils (CB[*n*]s, *n* = 5–8, 10) are a family of pumpkin-like macrocyclic hosts. CB[*n*] compounds bear a hydrophobic cavity and two identical portals surrounded by negative carbonyl groups as structural features, and have potential applications in many fields.[26–29] Similar to other hosts, CB[*n*]s have also been employed to promote various organic reactions, especially photodimerization reactions,[30–32] but have

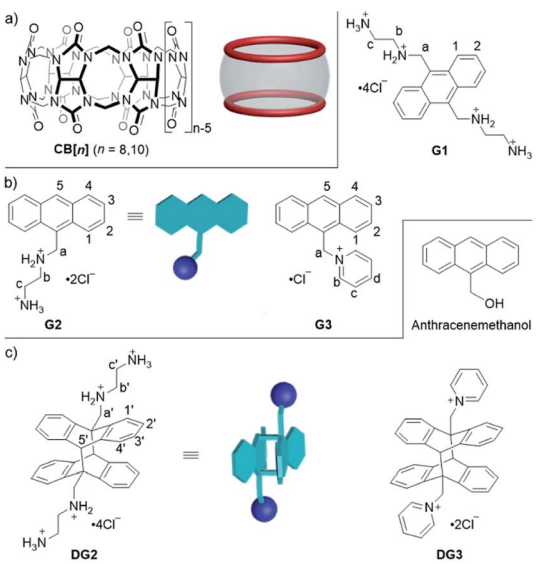

Fig. 1 Structures of (a) hosts CB[*n*] (*n* = 8, 10), (b) guests **G1–G3**, and (c) photoreaction products.

[a]*The State Key Laboratory of Refractories and Metallurgy, School of Chemistry and Chemical Engineering, Wuhan University of Science and Technology, Wuhan 430081, China. E-mail: liusimin@wust.edu.cn*

[b]*Institute of Advanced Materials and Nanotechnology, Wuhan University of Science and Technology, Wuhan 430081, China*

† Electronic supplementary information (ESI) available: Experimental details, binding ^{1}H NMR spectra, UV/Vis spectra of guests with CB[*n*], and relevant COSY, ESI-MS, ^{13}C NMR spectra, kinetics fitting. See DOI: 10.1039/d0sc00409j

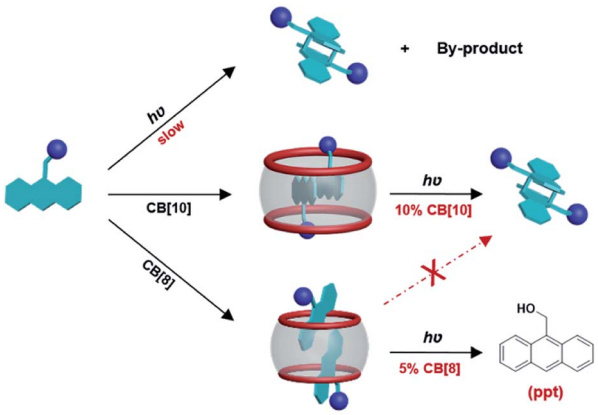

Scheme 1 Schematic illustration of CB[*n*]-mediated photoreactions of 9-substituted anthracene derivative **G2**.

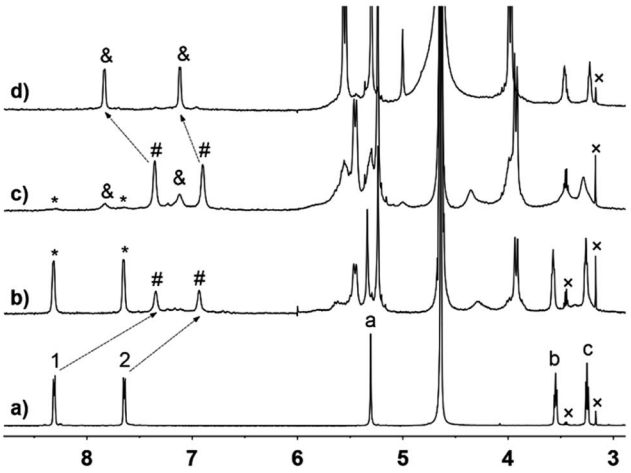

Fig. 2 ^{1}H NMR spectra (600 MHz, D_2O, 298 K): of (a) free **G1** (2.5 mM); (b) 4 : 1 mixture of **G1** and CB[10]; (c) 2 : 1 mixture of **G1** and CB[10]; (d) **G1** and excess CB[10] (resonances of free **G1** are marked with '*'; resonances of CB[10]·2**G1** are marked with '#', resonances of CB[10]·**G1** are marked with '&'; proton signals of impurities are marked with '×').

acted as supramolecular catalysts in only a few examples because the product is usually "trapped" in the CB[*n*] cavity, inhibiting the catalytic process.[33,34]

In this work, we investigated host–guest complexation between CB[*n*] (n = 8, 10) and 9-(10-)substituted anthracene derivatives (**G1**–**G3**) (Fig. 1) in aqueous solution, and the CB[*n*]-mediated (n = 8, 10) photoreaction of these guests. Notably, macrocyclic host-promoted photoreactions of 9-(10-)substituted anthracene derivatives have not been reported previously.[35–39] Our results showed that CB[10] and CB[8] had no obvious effects on the photoreaction of **G1**, despite encapsulating **G1**. However, for **G2** and **G3**, CB[10] operated as either a nanoreactor or catalyst (10%) for the photodimerization of two compounds with high selectivity and high yield. Although CB[8] formed a 1 : 2 complex with **G2**, as also observed with CB[10], photosolvolysis of **G2** was unexpectedly observed instead of dimerization after photoirradiation of the CB[8]·2**G2** complex (Scheme 1). A plausible reaction mechanism referring to anthracene as a PPG is provided.

Results and discussion

Complexation of G1 with CB[*n*] and photoreactions of complexes

Initially, the host–guest complexation of **G1** with CB[*n*] (n = 8, 10) was investigated by NMR, UV/Vis, and fluorescence spectroscopy, and ESI-MS analysis. ^{1}H NMR titration experiments clearly demonstrated the formation of host–guest complexes CB[10]·**G1** and CB[10]·2**G1**. As shown in Fig. 2b, binding between **G1** and CB[10] exhibited slow exchange kinetics on the ^{1}H NMR time scale, because both free and bound proton signals were observed. The slow exchange kinetics also allowed the binding ratio to be calculated as 1 : 2 (host/guest) from the integrals for peaks of bound guest and host. When the amount of CB[10] added was increased to 0.5 equiv. (Fig. 2c), a new set of bound guest peaks (marked as '&') was observed, along with a tiny amount of free guest (marked as '*'). Clearly the new inclusion complex also exhibited slow exchange kinetics on the ^{1}H NMR time scale. When excess CB[10] was added to a solution of **G1** (free CB[10] is insoluble in water and complexation with the guest usually allows CB[10] to enter the aqueous phase[40]), we calculated the binding ratio of CB[10] with **G1** to be 1 : 1, according to ^{1}H NMR peak integration (Fig. 2d). ESI-MS also indicated the existence of two inclusion complexes, CB[10]·**G1** and CB[10]·2**G1**. As shown in Fig. S1a,† ion peaks at m/z 577.5, 769.6, and 781.6 were observed, corresponding to 1 : 2 complex CB[10]·2**G1** ($[\mathrm{CB[10]} + 2\mathbf{G1}^{4+} - 4\mathrm{H}^+]^{4+} = 577.5$; $[\mathrm{CB[10]} + 2\mathbf{G1}^{4+} - 5\mathrm{H}^+]^{3+} = 769.6$; $[\mathrm{CB[10]} + 2\mathbf{G1}^{4+} - 4\mathrm{H}^+ + \mathrm{Cl}^-]^{3+} = 781.6$). The ion peak at m/z 996.4, corresponding to 1 : 1 complex CB[10]·**G1**, was also observed ($[\mathrm{CB[10]} + \mathbf{G1}^{4+} - 2\mathrm{H}^+]^{2+} = 996.4$) (Fig. S1†).

UV/Vis and fluorescence titrations were used to examine the complexation of CB[10] with **G1** in aqueous solution. With the addition of CB[10], the long-wavelength absorption of free **G1** at λ_{max} = 373 nm showed a bathochromic shift (Fig. S2†). In the absence of CB[10], **G1** showed the anthracene emission with a maximum wavelength of 422 nm. The fluorescence intensity of **G1** changed when CB[10] was added continuously, owing to host–guest complexation of **G1** with the CB[10] host (Fig. 3).[41] Furthermore, before the amount of CB[10] was increased to ~0.5 equiv., the fluorescence intensity of **G1** was observed to continuously decrease. However, at 1.0 equiv., the intensity increased about two-fold compared with that of **G1** itself, with a slight redshift. Combined with the NMR data, we speculated that CB[10] initially increased π–π stacking of **G1** by encapsulating two guest molecules in the cavity, causing fluorescence quenching through formation of the H-dimer of **G1**.[42] The further formation of 1 : 1 inclusion complex CB[10]·**G1** prevented **G1** from stacking and exterior aqueous environment, resulting in a stronger **G1** emission.[41] Meanwhile, host–guest complexation between CB[8] and **G1** was examined by ^{1}H NMR (Fig. S3†) and ESI-MS (Fig. S4†). Broadening of all proton signals, including those of CB[8], was observed when the amount of CB[8] was 0.5 equiv. (Fig. S3c†), indicating that

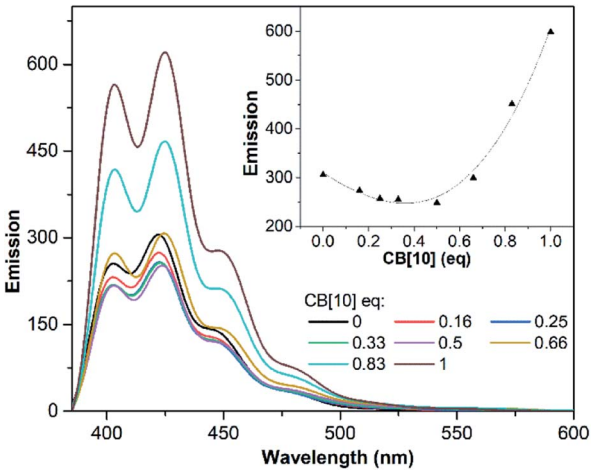

Fig. 3 Fluorescence emission spectra recorded for **G1** (31.25 μM) upon titration with CB[10]. Inset: emission of **G1** *vs.* CB[10] equivalent (λ_{ex} = 250 nm, λ_{em} = 422 nm).

binding between CB[8] and **G1** underwent intermediate exchange on the ^{1}H NMR time scale.[43] ESI-MS showed one ion peak at *m*/*z* 826.2, corresponding to 1 : 1 complex CB[8]·**G1** ([CB[8] + **G1**$^{4+}$ − 2H$^+$]$^{2+}$ = 826.2).

With the binding results in hand, we checked the photoreactions of **G1** in the absence and presence of CB[*n*] (*n* = 8, 10). Prior to UV irradiation at room temperature, all samples (in D_2O or pure water) were degassed with nitrogen for 15 min ([G] = 2.5 mM), and the reaction was monitored by ^{1}H NMR and UV/Vis spectroscopy. As shown in Fig. S5a,† the photoproducts of **G1** were complicated and unidentified. In the presence of 0.25 or 0.5 equiv. of CB[10], ratios which benefitted the dimerization reaction, the dimerization product was not observed as expected (Fig. S5b and c†). Molecular modeling (MMFF) suggested two **G1** molecules could adopt an "X" shape in the CB[10]·2**G1** complex owing to electrostatic repulsion between the 9,10-substituted positive groups (Fig. 4),[43] which was not a "reaction ready" state for dimerization. Similar results were obtained for the photoreaction of **G1** with various contents of CB[8]. Therefore, guest **G2** containing one substituent at the 9-position was designed.

Complexation of G2 with CB[*n*] and photoreactions of complexes

Similar to **G1**, we first investigated the host–guest complexation of **G2** with CB[*n*] hosts, and then conducted the photoreaction of **G2** with/without CB[*n*] (*n* = 8, 10). ^{1}H NMR titrations showed that the aromatic proton and H_a signals of **G2** were shifted upfield ($\Delta\delta$ = 0.97, 0.87, 0.97, 1.28, 1.05, and 1.63 ppm for protons H_1–H_5 and H_a, respectively) more than the H_b and H_c proton signals ($\Delta\delta$ = 0.47 and 0.28 ppm, respectively) by at least 0.40 ppm, suggesting that the anthracene moiety had advanced deeper and that the substituent was located around the portals of CB[10] (Fig. S6†). Broadening of the guest signals again implied that the binding of CB[10] and **G2** underwent intermediate exchange on the ^{1}H NMR time scale.[43] Upon adding excess CB[10], the ratio of CB[10] to **G2** was calculated to be 1 : 2 based on the integrals of the host and guest signals (Fig. S6c†). ESI-MS data further confirmed the formation of 1 : 2 complex CB[10]·2**G2**. As shown in Fig. S7,† an ion peak was observed at *m*/*z* 1081.9, which corresponded to the 1 : 2 complex ([CB[10] + 2**G2**$^{2+}$ − 2H$^+$]$^{2+}$ = 1081.9). UV/Vis and fluorescence titration experiments also corroborated the host–guest interaction of **G2** and CB[10] in the aqueous phase. The fluorescence emission intensity of **G2** decreased upon adding 0.5 equiv. of CB[10] (Fig. S8†), suggesting the existence of π–π stacking between the encapsulated anthracene units of **G2**, similar to that of **G1**. Interestingly, compared with **G1**, the binding of monosubstituted **G2** with CB[8] exhibited slow exchange kinetics on the ^{1}H NMR time scale, allowing the binding ratio to be calculated as 1 : 2 (host/guest) through integration (Fig. S9†). This

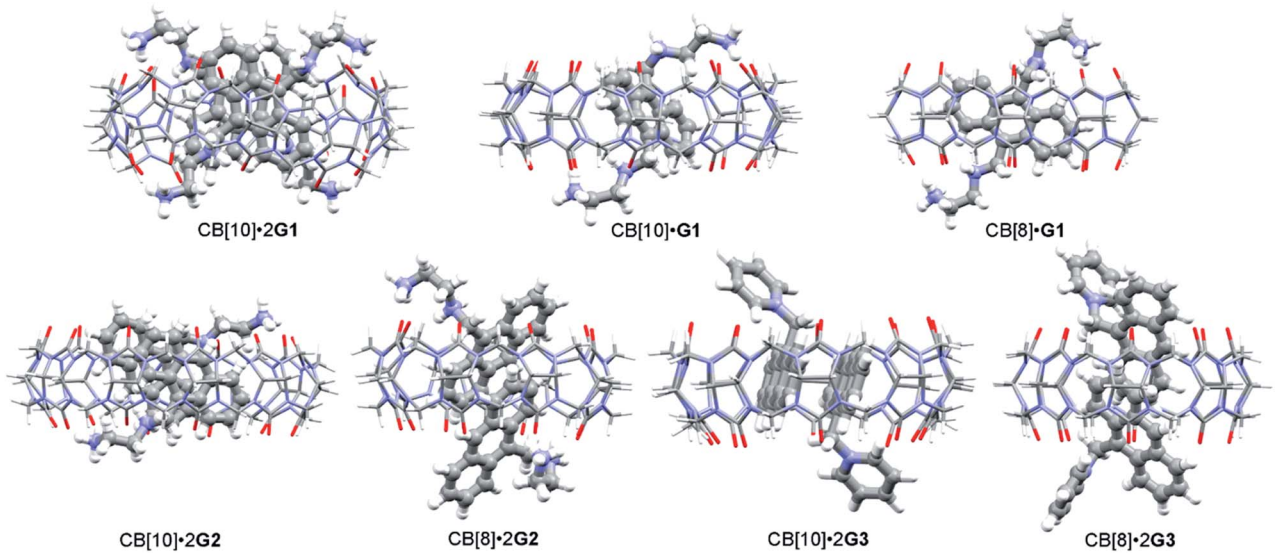

Fig. 4 Plausible binding modes of guests with CB[*n*] (MMFF-minimized).

1 : 2 binding was further verified by ESI-MS (Fig. S10†). The differentiation of proton signals on the left and right phenyl rings in **G2**, and no splits in the proton signals of CB[8] under slow exchange kinetics, suggested that the anthracene moieties were inserted into the cavity of CB[8] with the two incorporated **G2** molecules adopting a head-to-tail (h–t) orientation. Indeed, the MMFF-minimized model of complex CB[8]·2**G2** showed partial aromatic rings of two **G2** molecules located in the CB[8] cavity. The dihedral angle between the plane of the included anthracene group and the equatorial plane of CB[8] was about 59° (Fig. 4 and S11†). The distance between two included parallel anthracene groups was about 3.42 Å, suggesting the presence of π–π stacking.

Under the same conditions as for **G1**, photoreactions of **G2** were conducted in the absence and presence of CB[*n*] (*n* = 8, 10). As shown in Fig. S12,† after UV irradiation for 6 h, h–t dimer product **DG2** (purified and identified by irradiating complex CB[10]·2**G2**) was observed with unidentified side products and unreacted **G2**. In comparison, in the presence of 0.5 equiv. of CB[10], almost 100% of **G2** was converted into a single product within 25 min. As shown in Fig. 5b, under UV irradiation for 10 min, **G2** was partially converted into presumed new photoproduct(s). **G2** was consumed after 25 min, with only one set of CB[10] host and bound product(s) peaks remaining (Fig. 5c). After the appropriate amount of 3,5-dimethylamantadine hydrochloride (3,5-DMADA) was added to the irradiated solution of CB[10]·2**G2** to displace the product(s) from the CB[10] cavity (CB[10]·2(3,5-DMADA) is insoluble in water[44]), only one exclusive product, characterized as h–t dimer **DG2**, was obtained in almost quantitative yield (characterization data for **DG2** is shown in Fig. S13–S15 in ESI†). By monitoring absorbance changes of **G2** at λ = 370 nm, we calculated the yields of **DG2** with various irradiation times. As "the intra-complex photodimerization is unimolecular in nature",[18] an apparent rate constant (k_1) of 0.1158 ± 0.0079 min^{-1} for the dimerization reaction of **G2** with 50% CB[10] was calculated with first-order kinetics (Fig. S16†). The half-conversion time ($t_{1/2}$, time for conversion of half the substrate) was used because the rate constant could not be accurately measured in some cases. Clearly, in the presence of 50% CB[10], the dimerization reaction of **G2** was accelerated tremendously (Table 1). The high conversion, high selectivity, and rate acceleration of this photoreaction of **G2** within CB[10] suggested that two **G2** molecules were preorganized by CB[10] to adopt a "reaction ready" h–t orientation, which was in good agreement with the MMFF-minimized model of complex CB[10]·2**G2** in Fig. 4.

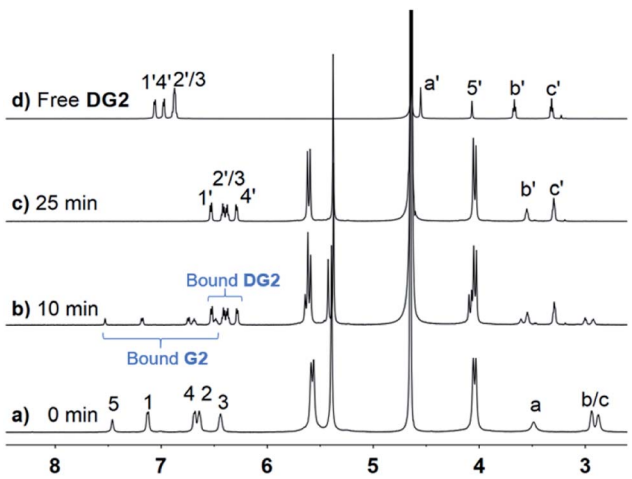

Fig. 5 ^{1}H NMR spectra (600 MHz, D_2O, 298 K) of CB[10]·2**G2** ([**G2**] = 2.5 mM) solution with various UV irradiation times: (a) 0, (b) 10, (c) 25 min, and (d) free dimerization product **DG2**.

Table 1 Half-conversion time ($t_{1/2}$) for guests with/without CB[*n*] (*n* = 8, 10) in water at 298 K

Host	$t_{1/2}$ (**G2**)	$t_{1/2}$ (**G3**)
None	1.7 h[a]	7.5 h[a]
CB[10] (50%)	6 min[b]	37 min[b]
CB[10] (10%)	44 min[b]	110 min[b]
CB[8] (50%)	8 min[c]	—[d]
CB[8] (5%)	35 min[c]	—[d]

[a] Estimated from NMR integrals (Fig. S12 and S32). [b] Calculated by fitting equation (Fig. S16, S18 and S39). [c] Estimated from diagrams of product yields (Fig. S26). [d] Not determined.

Inspired by a previous sample,[33] we investigated whether CB[10] could act as a supramolecular catalyst to convert **G2** into **DG2** exclusively. In the presence of 0.1 equiv. of CB[10] (10%), almost 100% of **G2** was converted into photoproduct **DG2** with trace amounts of side products within 120 min (Fig. S17†). The $t_{1/2}$ of 44 min was calculated from the first-order kinetics equation (Fig. S18†). In comparison, the $t_{1/2}$ of **G2** without CB[10] was estimated to be 1.7 hours (Table 1). All data suggested that CB[10] operated as the supramolecular catalyst in this case, although the photoreaction took longer to achieve than that with 0.5 equiv. of CB[10] (Scheme 1). As mentioned above, effective replacement of the product (**DG2**) with the starting material (**G2**) was necessary for host (CB[10]) to operate as a catalyst. To verify this, ^{1}H NMR competition experiments between **DG2** and **G2** with CB[10] were performed.

As predicted, the mixture of **G2**, **DG2**, and CB[10] with a 2 : 1 : 1 ratio resulted in most CB[10] being occupied by **G2** (Fig. S19c†). An approximate equilibrium constant (K_{eq}) was calculated as 8.8×10^5 M^{-1} (Fig. S20 and S21†), suggesting that CB[10] operated as a supramolecular catalyst owing to the spontaneous replacement of product **DG2** with starting material **G2**. The results showed that, as either the supramolecular nanoreactor or catalyst, CB[10] not only shortened the photoreaction time, but also tremendously improved the reaction selectivity.

When the host molecule was switched to CB[8], an unexpected photoreaction of **G2** occurred, although CB[8] bound **G2** with the same binding ratio as CB[10]. In the presence of 0.5 equiv. of CB[8], precipitate formation was observed when the **G2** solution was irradiated with UV light. With extended irradiation time, additional yellow precipitate was generated. Therefore, the solutions after centrifugation were carefully monitored by ^{1}H NMR. By analyzing the stacking NMR spectra (Fig. 6) and the precipitate, the bound peaks of **G2** were found to fully disappear in 60 min, while a singlet peak at 3.1 ppm appeared and

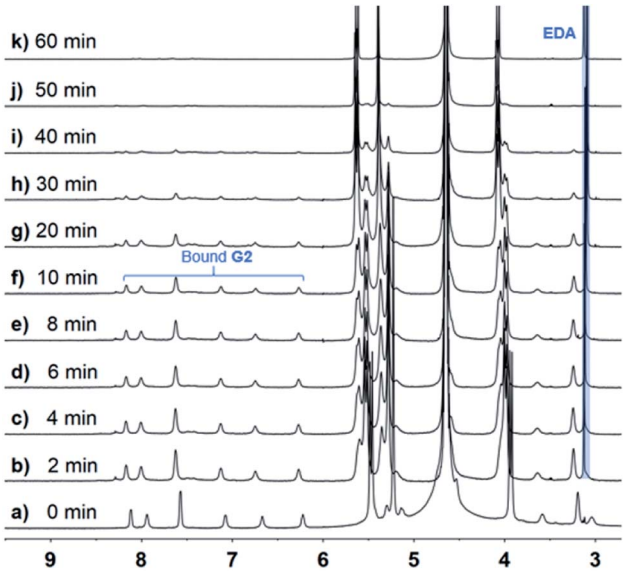

Fig. 6 ^{1}H NMR spectra (600 MHz, D_2O, 298 K) of 2 : 1 mixture of **G2** (2.5 mM) and CB[8] with various UV irradiation times.

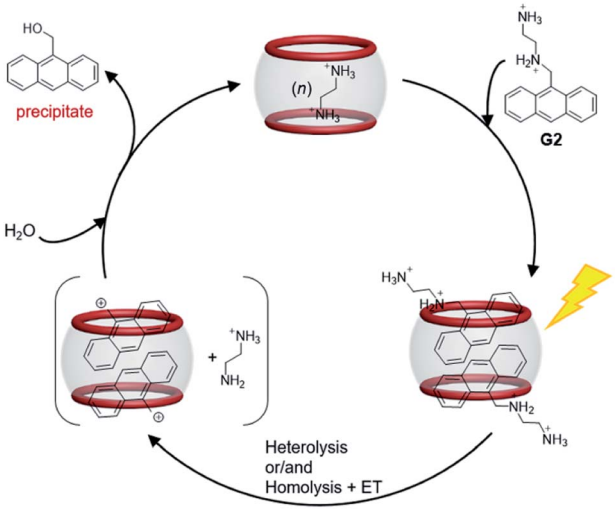

Scheme 2 Plausible reaction mechanism for the photosolvolysis reaction of **G2** in the presence of CB[8] host (5%).

remained, and the yellow precipitate contained no CB[8] and was soluble in DMSO and $CDCl_3$. First, we suspected that the precipitate was anthraquinone, because anthracene derivatives can easily be oxidized,[45,46] despite the photoreaction being conducted under N_2 atmosphere. However, the NMR signals for the precipitate did not match those of anthraquinone. Further hypotheses included the photosolvolysis of **G2**. Eventually, the yellow precipitate was verified to be 9-anthracenemethanol by EI-MS and ^{1}H NMR (Fig. S22a and S23†). When irradiated in air, **G2** first generated 9-anthracenemethanol as a precipitate (suspended), which was then converted to anthraquinone (Fig. S22b†), further confirming the occurrence of photosolvolysis prior to photooxidation. The singlet peak in the aqueous phase represented the ethylene proton signal of ethylenediamine (EDA). And the binding of protonated EDA in CB[8] helped solubilize CB[8] in water at high concentrations (maximum solubility of CB[8] in water is about 0.2 mM). Indeed, NMR titration experiments proved that small EDA molecules could be encapsulated by CB[8] (Fig. S24†). Furthermore, CB[8] was tested to determine whether it could act as a supramolecular catalyst in the photosolvolysis of **G2**. In the presence of 0.05 equiv. of CB[8] (5%), **G2** was almost all converted to 9-anthracenemethanol within 4 h (Fig. S25†). In comparison, no precipitate was observed without CB[8]. The $t_{1/2}$ of **G2** in the presence of CB[8] was estimated because the data could not be ideally fitted with first-order kinetics (Table 1 and Fig. S26†). CB[8] doubtless operated as a supramolecular catalyst for the photosolvolysis of **G2**. Therefore, why photosolvolysis occurred when **G2** itself did not show the same reactivity required further investigation.

After a broad search of the photosolvolysis literature, we noted that a "photoremovable protecting group (PPG)" could be involved in this reaction.[12,47] To date, only one example of an anthracene unit acting as a PPG has been reported, with the plausible mechanism involving heterolysis and/or homolysis of the CH_2–X bond in PPG–CH_2–X (X, leaving group) to produce a carbonium ion intermediate. CB[*n*] hosts are known to be capable of stabilizing active carbocations.[34,48,49] Therefore, a plausible mechanism for the photosolvolysis of **G2** with CB[8] as the supramolecular catalyst in aqueous solution was proposed. As shown in Scheme 2, the initial step is light-induced heterolytic cleavage of the C–N bond of encapsulated **G2**, and/or homolytic cleavage of the C–N bond followed by rapid electron transfer (ET), to give the carbonium ion intermediate and EDA. The CB[8]-stabilized carbonium ion is then attacked by solvent molecule H_2O to give product 9-anthracenemethanol. Owing to its weak binding with CB[8] and insolubility, 9-anthracenemethanol is displaced by **G2** or EDA and precipitated out of solution, allowing the catalytic process to continue. Compared with the observation of radical side products (caused by homolysis) in most reported examples,[12] the generation of a single product with quantitative yield in this case suggested that, with the assistance of CB[8], either C–N bond heterolysis was favored over homolysis or the electron transfer step after homolysis was accelerated.

The high conversion and high selectivity of this photosolvolysis of **G2** suggested that the orientation of the two **G2** molecules in CB[8] was not only unfavorable for dimerization, but also favorable for stabilization of the carbonium ion intermediate by CB[8]. In addition to acting as the supramolecular catalyst, the most interesting role of CB[8] in this case was efficiently switching the reaction pathway of **G2** from familiar photodimerization to unusual photosolvolysis.

Complexation of G3 with CB[*n*] and photoreactions of complexes

Guest molecule **G3** was synthesized to explore the effect of different substituent groups on the photochemical reaction. The host–guest complexation of **G3** with CB[*n*] (n = 8, 10) was investigated by ^{1}H NMR, UV/Vis, and fluorescence spectroscopy, and ESI-MS analysis (Fig. S27–S31†). The ESI-MS data indicated

that the complexation ratio of CB[*n*] with **G3** was 1 : 2 (ion peaks at *m*/*z* 1100.9 and 934.8 corresponding to 1 : 2 complexes CB[10]·2**G3** and CB[8]·2**G3**, respectively) (Fig. S29 and S31†). Similar to **G2**, the photoreaction of **G3** slowly produced h–t dimerization product **DG3** and unidentified side products (Fig. S32†). Furthermore, the dimerization of **G3** with CB[10] operating as a supramolecular nanoreactor and catalyst, exclusively gave **DG3** (Fig. S33–S39†). No bound peaks of **DG3** were observed in the NMR competition experiments, indicating that the binding of **G3** with CB[10] was much stronger than that of **DG3** (Fig. S38†). The dimerization reaction of **G3** was also greatly accelerated with assistance from CB[10] (Table 1 and Fig. S39†). However, in the presence of CB[8], no precipitate and an extremely complicated ^{1}H NMR spectrum of photoproducts were observed, suggesting the negative effect of CB[8] on the photoreaction of **G3** (Fig. S40†). It is unclear whether the lack of photosolvolysis of **G3** was due to the deactivating effect of the pyridinium substituent group or the unfavorable orientation of **G3** in CB[8].

Conclusions

In summary, we have reported the effects of CB[*n*] (n = 8, 10) hosts on the photoreaction of 9-(10-)anthracene derivatives. Both CB[8] and CB[10] operated as supramolecular nanoreactors and catalysts in the photoreaction of 9-substituted anthracene derivative **G2**. However, CB[10] promoted the photodimerization of **G2**, which occurred slowly with lower selectivity without a host. In contrast, CB[8] exclusively induced the photosolvolysis of **G2**, which did not occur without a host. Furthermore, the photoreactions of two anthracene derivatives, **G1** and **G3**, were investigated in the presence of CB[*n*] to compare the effect of different CB[*n*] on the reactivity of anthracene derivatives with various substituents. The results showed that small differences in the host structures could cause large different effects on the host-involved reaction selectivity.

As the first example of CB[10] operating as a supramolecular nanoreactor/catalyst, we anticipate that more reactions, involving large-sized or more than two substrate molecules, can be promoted by the large cavity of CB[10]. The selectivity for photosolvolysis of aromatic substrates with a PPG is also expected to be improved by the ability of CB[*n*] to stabilize cations. These finding will further benefit CB[*n*] chemistry and supramolecular catalysis.

Conflicts of interest

There are no conflicts to declare.

Acknowledgements

This work was financially supported by the National Natural Science Foundation of China (21871216, 21472143).

Notes and references

1 P. W. N. M. van Leeuwen, in *Supramolecular catalysis*, Wiley-VCH, 2008.
2 J. Meeuwissen and J. N. H. Reek, *Nat. Chem.*, 2010, **2**, 615–621.
3 U. H. Brinker and J.-L. Mieusset, in *Molecular Encapsulation Organic Reactions in Constrained Systems*, Wiley, 2010, pp. 43–115.
4 P. Neri, J. L. Sessler and M.-X. Wang, in *Calixarenes and beyond*, Springer, 2016, pp. 691–742.
5 E. H. Wanderlind, D. G. Liz, A. P. Gerola, R. F. Affeldt, V. Nascimento, L. C. Bretanha, R. Montecinos, L. Garcia-Rio, H. D. Fiedler and F. Nome, *ACS Catal.*, 2018, **8**, 3343–3347.
6 M. Yoshizawa, J. K. Klosterman and M. Fujita, *Angew. Chem., Int. Ed.*, 2009, **48**, 3418–3438.
7 S. Zarra, D. M. Wood, D. A. Roberts and J. R. Nitschke, *Chem. Soc. Rev.*, 2015, **44**, 419–432.
8 A. Galan and P. Ballester, *Chem. Soc. Rev.*, 2016, **45**, 1720–1737.
9 S. Sadjadi, in *Organic Nanoreactors: From Molecular to Supramolecular Organic Compounds*, Academic Press, 2016.
10 H. D. Becker, *Chem. Rev.*, 1993, **93**, 145–172.
11 H. Bouas-Laurent, A. Castellan, J.-P. Desvergne and R. Lapouyade, *Chem. Soc. Rev.*, 2000, **29**, 43–55.
12 P. Klán, T. Šolomek, C. G. Bochet, A. Blanc, R. Givens, M. Rubina, V. Popik, A. Kostikov and J. Wirz, *Chem. Rev.*, 2013, **113**, 119–191.
13 A. K. Singh and P. K. Khade, *Tetrahedron Lett.*, 2005, **46**, 5563–5566.
14 H. Wang, F. Liu, R. C. Helgeson and K. N. Houk, *Angew. Chem., Int. Ed.*, 2013, **52**, 655–659.
15 A. Tron, H.-P. Jacquot de Rouville, A. Ducrot, J. H. R. Tucker, M. Baroncini, A. Credi and N. D. McClenaghan, *Chem. Commun.*, 2015, **51**, 2810–2813.
16 J.-C. Gui, Z.-Q. Yan, Y. Peng, J.-G. Yi, D.-Y. Zhou, D. Su, Z.-H. Zhong, G.-W. Gao, W.-H. Wu and C. Yang, *Chin. Chem. Lett.*, 2016, **27**, 1017–1021.
17 X. Wei, W. Wu, R. Matsushita, Z. Yan, D. Zhou, J. J. Chruma, M. Nishijima, G. Fukuhara, T. Mori, Y. Inoue and C. Yang, *J. Am. Chem. Soc.*, 2018, **140**, 3959–3974.
18 J. Ji, W. Wu, W. Liang, G. Cheng, R. Matsushita, Z. Yan, X. Wei, M. Rao, D.-Q. Yuan, G. Fukuhara, T. Mori, Y. Inoue and C. Yang, *J. Am. Chem. Soc.*, 2019, **141**, 9225–9238.
19 J.-F. Xu, Y.-Z. Chen, L.-Z. Wu, C.-H. Tung and Q.-Z. Yang, *Org. Lett.*, 2013, **15**, 6148–6151.
20 P. Wei, X. Yan and F. Huang, *Chem. Commun.*, 2014, **50**, 14105–14108.
21 X. Zhang, Y. Gao, Y. Lin, J. Hu and Y. Ju, *Polym. Chem.*, 2015, **6**, 4162–4166.
22 W. Guan, G. Wang, J. Ding, B. Li and L. Wu, *Chem. Commun.*, 2019, **55**, 10788–10791.
23 Q. Zhou, B. Zhang, D. Han, R. Chen, F. Qiu, J. Wu and H. Jiang, *Chem. Commun.*, 2015, **51**, 3124–3126.
24 W. Zhou, Y. Chen, Q. Yu, P. Li, X. Chen and Y. Liu, *Chem. Sci.*, 2019, **10**, 3346–3352.
25 M. Tu, H. Reinsch, S. Rodríguez-Hermida, R. Verbeke, T. Stassin, W. Egger, M. Dickmann, B. Dieu, J. Hofkens, I. F. J. Vankelecom, N. Stock and R. Ameloot, *Angew. Chem., Int. Ed.*, 2019, **58**, 2423–2427.

26 J. Lagona, P. Mukhopadhyay, S. Chakrabarti and L. Isaacs, *Angew. Chem., Int. Ed.*, 2005, **44**, 4844–4870.
27 E. Masson, X. Ling, R. Joseph, L. Kyeremeh-Mensah and X. Lu, *RSC Adv.*, 2012, **2**, 1213–1247.
28 S. J. Barrow, S. Kasera, M. J. Rowland, J. del Barrio and O. A. Scherman, *Chem. Rev.*, 2015, **115**, 12320–12406.
29 X. Yang, F. Liu, Z. Zhao, F. Liang, H. Zhang and S. Liu, *Chin. Chem. Lett.*, 2018, **29**, 1560–1566.
30 K. I. Assaf and W. M. Nau, *Chem. Soc. Rev.*, 2015, **44**, 394–418.
31 S. Sadjadi, in *Organic Nanoreactors: From Molecular to Supramolecular Organic Compounds*, Elsevier, 2016, pp. 43–84.
32 K. Kim, in *Cucurbiturils and Related Macrocycles*, The Royal Society of Chemistry, 2019, pp. 86–120.
33 Y. Kang, X. Tang, H. Yu, Z. Cai, Z. Huang, D. Wang, J.-F. Xu and X. Zhang, *Chem. Sci.*, 2017, **8**, 8357–8361.
34 L. Scorsin, J. A. Roehrs, R. R. Campedelli, G. F. Caramori, A. O. Ortolan, R. L. T. Parreira, H. D. Fiedler, A. Acuña, L. García-Río and F. Nome, *ACS Catal.*, 2018, **8**, 12067–12079.
35 C. Yang, T. Mori, Y. Origane, Y. H. Ko, N. Selvapalam, K. Kim and Y. Inoue, *J. Am. Chem. Soc.*, 2008, **130**, 8574–8575.
36 F. Biedermann, I. Ross and O. A. Scherman, *Polym. Chem.*, 2014, **5**, 5375–5382.
37 C. P. Carvalho, Z. Domínguez, J. P. Da Silva and U. Pischel, *Chem. Commun.*, 2015, **51**, 2698–2701.
38 C.-H. Tung and J.-Q. Guan, *J. Org. Chem.*, 1998, **63**, 5857–5862.
39 D.-Y. Wu, B. Chen, X.-G. Fu, L.-Z. Wu, L.-P. Zhang and C.-H. Tung, *Org. Lett.*, 2003, **5**, 1075–1077.
40 W. Gong, X. Yang, P. Y. Zavalij, L. Isaacs, Z. Zhao and S. Liu, *Chem.–Eur. J.*, 2016, **22**, 17612–17618.
41 R. N. Dsouza, U. Pischel and W. M. Nau, *Chem. Rev.*, 2011, **111**, 7941–7980.
42 N. Barooah, J. Mohanty and A. C. Bhasikuttan, *Chem. Commun.*, 2015, **51**, 13225–13228.
43 X. Zhao, F. Liu, Z. Zhao, H. Karoui, D. Bardelang, O. Ouari and S. Liu, *Org. Biomol. Chem.*, 2018, **16**, 3809–3815.
44 X. Yang, Z. Zhao, X. Zhang and S. Liu, *Sci. China: Chem.*, 2018, **61**, 787–791.
45 K. I. Assaf, M. A. Alnajjar and W. M. Nau, *Chem. Commun.*, 2018, **54**, 1734–1737.
46 P. Anzenbacher, T. Niwa, L. M. Tolbert, S. R. Sirimanne and F. P. Guengerich, *Biochemistry*, 1996, **35**, 2512–2520.
47 P. Wang, *Asian J. Org. Chem.*, 2013, **2**, 452–464.
48 R. Wang and D. H. Macartney, *Tetrahedron Lett.*, 2008, **49**, 311–314.
49 N. Basilio, L. García-Río, J. A. Moreira and M. Pessêgo, *J. Org. Chem.*, 2010, **75**, 848–855.